

UC Davis

UC Davis Previously Published Works

Title

On measuring the response of mesophyll conductance to carbon dioxide with the variable J method.

Permalink

<https://escholarship.org/uc/item/00c8b4np>

Journal

Journal of experimental botany, 63(1)

ISSN

0022-0957

Authors

Gilbert, Matthew Edmund
Pou, Alcía
Zwieniecki, Maciej Andrzej
et al.

Publication Date

2012

DOI

10.1093/jxb/err288

Peer reviewed

RESEARCH PAPER

On measuring the response of mesophyll conductance to carbon dioxide with the variable J method

Matthew Edmund Gilbert^{1,*}, Alícia Pou², Maciej Andrzej Zwieniecki³ and N. Michele Holbrook¹

¹ Organismic and Evolutionary Biology, Harvard University, Cambridge, MA 02138, USA

² Grup de Recerca en Biologia de les Plantes en Condicions Mediterrànies, Departament de Biologia, Universitat de les Illes Balears, Carretera de Valldemossa Km 7.5, 07122 Palma de Mallorca, Balears, Spain

³ Arnold Arboretum, Harvard University, Cambridge, MA 02138, USA

* To whom correspondence should be addressed. E-mail: mgilbert@oeb.harvard.edu

Received 31 March 2011; Revised 5 August 2011; Accepted 15 August 2011

Abstract

The response of mesophyll conductance to CO_2 (g_m) to environmental variation is a challenging parameter to measure with current methods. The 'variable J ' technique, used in the majority of studies of g_m , assumes a one-to-one relationship between photosystem II (PSII) fluorescence and photosynthesis under non-photorespiratory conditions. When calibrating this relationship for *Populus trichocarpa*, it was found that calibration relationships produced using variation in light and CO_2 were not equivalent, and in all cases the relationships were non-linear—something not accounted for in previous studies. Detailed analyses were performed of whether different calibration procedures affect the observed g_m response to CO_2 . Past linear and assumed calibration methods resulted in systematic biases in the fluorescence estimates of electron transport. A sensitivity analysis on modelled data (where g_m was held constant) demonstrated that biases in the estimation of electron transport as small as 2% ($\sim 0.5 \mu\text{mol m}^{-2} \text{s}^{-1}$) resulted in apparent changes in the relationship of g_m to CO_2 of similar shape and magnitude to those observed with past calibration techniques. This sensitivity to biases introduced during calibrations leads to results where g_m artefactually decreases with CO_2 , assuming that g_m is constant; if g_m responds to CO_2 , then biases associated with past calibration methods would lead to overestimates of the slope of the relationship. Non-linear calibrations were evaluated; these removed the bias present in past calibrations, but the method remained sensitive to measurement errors. Thus measurement errors, calibration non-linearities leading to bias, and the sensitivity of variable J g_m hinders its use under conditions of varying CO_2 or light.

Key words: Chlorophyll fluorescence, curve fitting, electron transport rate, g_m , mesophyll conductance to CO_2 , *Populus trichocarpa*, variable J technique.

Introduction

Mesophyll conductance (g_m) is the conductance of CO_2 from the intercellular airspaces to Rubisco, a largely liquid pathway through the cell wall and three membranes. Whether g_m is a constitutive or dynamic characteristic of a leaf is fundamental to our understanding of plant responses to the environment. As g_m may represent up to

Abbreviations: α , leaf absorptance; β , fraction of quanta absorbed by PSII; Φ_{PSII} , quantum efficiency of PSII; Φ_{CO_2} , quantum efficiency of gas exchange; Γ^* , photo-compensation point; A , net photosynthetic rate; A_c , Rubisco-limited photosynthetic rate; A_p , RuBP regeneration-limited photosynthetic rate; A_{TPU} , triose phosphate utilization-limited photosynthetic rate; C_c , chloroplastic CO_2 concentration; C_i , intercellular CO_2 concentration; C_i^* , apparent photo-compensation point; EDO, exhaustive dual optimization procedure; g_m , mesophyll conductance to CO_2 ; K_c , Rubisco Michaelis–Menten constant for carboxylation; K_o , Rubisco Michaelis–Menten constant for photorespiration; J , electron transport rate; J_{A+R} , rate of J needed to account for measured $A+R$; J_{cal} , calibrated fluorescence-derived J ; J_{RAW} , uncalibrated fluorescence-derived J ; J_{total} , modelled or measured total J to carboxylation and photorespiration; O , oxygen mole fraction; PPFD, photosynthetic photon flux density; R_d , mitochondrial respiration in the light; $S_{c/o}$, relative specificity of Rubisco; T_l , leaf temperature; V_c , rate of carboxylation; $V_{c,c}$, rate of carboxylation limited by Rubisco; $V_{c,j}$, rate of carboxylation limited by RuBP regeneration; $V_{c,\text{min}}$, minimum of $V_{c,c}$ and $V_{c,j}$; $V_{c,\text{max}}$, maximum rate of Rubisco carboxylation; V_o , rate of photorespiration; V_{alt} , alternative J in CO_2 equivalents; VPD, vapour pressure deficit.

© 2011 The Author(s).

This is an Open Access article distributed under the terms of the Creative Commons Attribution Non-Commercial License (<http://creativecommons.org/licenses/by-nc/3.0>), which permits unrestricted non-commercial use, distribution, and reproduction in any medium, provided the original work is properly cited.

40% of the CO₂ diffusional limitation on photosynthesis (Warren, 2008), dynamic variation in g_m would offer a major avenue for photosynthetic regulation, comparable with that of the stomata. The most commonly used technique to measure g_m , the variable J method, consistently demonstrates a large reduction in g_m with increasing CO₂ (Flexas *et al.*, 2007). However, the size and presence of the response of g_m to CO₂ varies between studies using a variety of methods (Flexas *et al.*, 2007; Tazoe *et al.*, 2009; Vrabl *et al.*, 2009). For example, a less steep response of g_m to CO₂ was found for *Nicotiana tabacum* using the independent carbon isotope method relative to the variable J method (Flexas *et al.*, 2007). In a separate experiment, *Arabidopsis thaliana* and *N. tabacum* were reported to reduce g_m by ~85% and 65%, respectively, when CO₂ changed from 200 $\mu\text{mol mol}^{-1}$ to 1000 $\mu\text{mol mol}^{-1}$ at 21% O₂ and measured using the variable J method (Flexas *et al.*, 2007). In a second investigation, the carbon isotope method resulted in only a 10% reduction and a 5% increase for the same species, respectively, when measured across the same range of CO₂ mole fractions; measurements at 2% O₂ showed reductions of 26% and 40% (Tazoe *et al.*, 2011). The widely used curve-fitting techniques for estimating g_m explicitly assume a constant g_m across the range of CO₂ used to generate CO₂ response curves (Ethier *et al.*, 2006; Warren, 2006; Sharkey *et al.*, 2007; Gu *et al.*, 2010). To date the underlying mechanisms determining g_m and the reason for the different results between methods remain unresolved.

The 'variable J ' technique encompasses a group of methods that estimate g_m , chloroplastic CO₂ concentration (C_c), and the rate of oxygenation or photorespiration (V_o) from combined fluorescence and gas exchange data. Mesophyll conductance to CO₂ is calculated as the ratio of net photosynthetic CO₂ flux (A) to the difference in CO₂ concentration between the intercellular airspaces (C_i) and the chloroplast (C_c). C_c is related to the ratio of carboxylation to photorespiration at Rubisco, and photorespiration is then proportional to the difference between fluorescence-derived estimates of the total electron transport rate and the rate of electron use by carboxylation estimated from gas exchange. This derivation is described in detail in the Materials and methods and reviewed by Warren (2006) and by Pons *et al.* (2009).

Fluorescence estimates of total electron transport are derived from the work of Genty *et al.* (1989), who established that under non-photorespiratory conditions (low oxygen and high CO₂), a linear relationship exists between the quantum yield of fluorescence (Φ_{PSII}) and measured quantum efficiency of rates of CO₂ fixation (Φ_{CO_2}). This proportionality has subsequently been used to provide an estimate of electron transport rates: in the absence of alternative electron sinks, the relationship between carboxylation estimates of linear electron flow and fluorescence estimates of electron transport should be one-to-one under non-photorespiratory conditions. In practice, this relationship deviates from one-to-one due to interspecific variation in the values of standard constants such as leaf absorptance (Baker, 2008), and measurement

of the relationship under non-saturating CO₂ where significant alternative electron transport sinks may be present. However, for simplicity, it is often assumed that standard constants are accurate and do not vary during experiments.

An alternative approach is to conduct pre-experimental calibrations to provide estimates of electron transport from photosystem II (PSII) fluorescence (Lawlor and Tezara, 2009). While empirical calibration has the potential to improve estimates of electron transport, it can also introduce systematic errors (biases) in the calculation of the total electron transport rate, and thus g_m . The impact of calibration issues, such as non-linearity, on the calculation of g_m has not been thoroughly assessed.

The present study examined whether the differences between two common methods used for measuring g_m is the result of biases in the calibration of the variable J method. However, the challenges inherent in the variable J method have long been recognized (Harley *et al.*, 1992), with the Harley criterion providing an indication of how sensitive the g_m values are to errors when using this method (Harley *et al.*, 1992). The original sensitivity analyses of Harley *et al.* (1992) demonstrated that the relationship of g_m to CO₂ was sensitive to errors in the values of mitochondrial respiration, the photo-compensation point, and the fluorescence estimate of the total electron transport rate. However, this analysis was not extended to a broad range of C_i s, as subsequent studies do, and the sensitivity of the g_m response to CO₂ to errors has not been compared with the size of biases present in the calibration procedure.

Therefore, the goal of this study was to understand the conditions under which g_m can be accurately measured using the variable J technique. Fluorescence with gas exchange measurements is calibrated using classical methods for the widely used genome model plant poplar (*Populus trichocarpa* Torr. & Gray). Consistent with the original literature, significant variation in the calibration relationship was found, such that there is the potential for systematic error when calibrations are applied to a broad range of environmental conditions. Photosynthetic models are then used to assess the effects of biases on the response of g_m to CO₂. Finally, new calibration techniques by which these biases may be reduced when estimating a single value of g_m for a leaf, or comparing species, are suggested. However, it is demonstrated that the variable J method should be used with caution when measuring the response of g_m to CO₂ and light, as any bias in the estimation of electron transport rates results in changes in the relationship of g_m with CO₂.

Materials and methods

Plant material and growing conditions

Poplar plants were propagated from cuttings and grown in environmentally controlled growth chambers. Metal-halide and high pressure sodium lighting (400 $\mu\text{mol m}^{-2} \text{s}^{-1}$) was provided for 14 h per day. Temperatures in the chambers were maintained

between 20 °C and 24 °C, and humidity was kept at 70%. The cuttings were placed in 3785 cm³ pots in Farfard 3B potting soil which included Osmocote Plus slow release fertilizer as per the manufacturer's instructions (15/9/12/1 N/P/K/Mg plus trace elements: S, B, Cu, Fe, Mn, Mo, and Zn; Scotts Company, OH, USA). The pots were watered daily and fertilized weekly with Peters Excel All Purpose soluble fertilizer (21/5/20 N/P/K plus trace elements: B, Cu, Fe, Mn, Mo, and Zn; Scotts Company). Plants were measured after 4–9 months of growth in March–May of 2010 (all experiments), and a second set of plants in November 2010 (extra CO₂ response curves).

Gas exchange and fluorescence measurements

Gas exchange and fluorescence measurements were done on young fully expanded leaves using a 2 cm² LI-COR LI-6400 fluorescence chamber and gas exchange system (LI-COR, Lincoln, NE, USA). Plants were allowed to acclimate to the gas exchange system in a laboratory growth chamber for >30 min, until stomatal conductance was stable. Unless otherwise noted, general measurement conditions were as follows: photosynthetic photon flux density (PPFD), 400 μmol m⁻² s⁻¹ with no blue light component (Loreto *et al.*, 2009); reference CO₂, 400 μmol mol⁻¹; T_l, 24.9±0.8 °C; vapour pressure deficit (VPD), 1.47±0.49 kPa; flow, 150 μmol s⁻¹. Single flash fluorescence measurement settings were used and adjusted according to the optimal values obtained from the flash and measuring intensity procedures in the LI-6400 manual (Anon, 2004). All measurements were corrected for leaks using empirically determined leak corrections for dry poplar leaves under measurement conditions (CO₂S_{corrected}=CO₂S_{uncorrected}+9.868×10⁻⁷×CO₂R²+5.291×10⁻⁴×CO₂R-1.008).

The Laik method was used to measure non-photorespiratory respiration in the light (*R_d*) and the apparent photo-compensation point (*C_i**) (Warren, 2006). In this method, the *y* and *x* value of the average intersection of three CO₂ responses are taken as *R_d* and *C_i**. The CO₂ responses were measured at reference CO₂ concentrations of 150, 100, 75, and 50 μmol mol⁻¹, at three light levels 400, 175, and 75 μmol m⁻² s⁻¹. Six replicate sets of measurements were made providing mean (±SD) values of 0.42±0.21 μmol m⁻² s⁻¹ for *R_d*, and 36.0±1.9 μmol mol⁻¹ for *C_i**. In theory, the *C_i** values should be increased by *R_d*/*g_m* to obtain an estimate of the photocompensation point *Γ** (von Caemmerer, 2000), but as no independent value for *g_m* was available, the transformation was not performed and *Γ** was taken to be equal to *C_i**. A sensitivity analysis, described below, confirmed that minor variation in the value for *Γ** did not greatly affect the values of *g_m* (Table 1).

Low oxygen, non-photorespiratory conditions, were obtained by mixing air with nitrogen gas using a Wösthoff gas mixer to achieve a 1% O₂ content. This was tested using CO₂ drawdown as an indicator of the 5% mixing ratio necessary to produce 1% O₂ from 21% O₂ air, and further verified using an Ocean Optics USB4000-FL-450 Fiber Optic Spectrophotometer oxygen probe. Initial experiments demonstrated that 1% O₂ was the highest oxygen concentration at which the slope of the variable *J* calibration relationship did not change with successive dilution of O₂ at ambient CO₂, indicating that further reductions in O₂ would not further inhibit photorespiration.

Calibration relationships and CO₂ responses

Light or CO₂ response curves were measured under non-photorespiratory conditions to calibrate the relationship between fluorescence-derived electron transport rates (*J_{raw}*) and photosynthesis (*J_{A+R_d}*). Nine light response curves were measured at ambient CO₂ (400 μmol mol⁻¹) and 1% O₂, starting at a PPFD of 2000 μmol m⁻² s⁻¹ and reducing PPFD to 1500, 1000, 800, 600, 500, 400, 350, 300, 250, 200, 150, and 100 μmol m⁻² s⁻¹ with 4–6 min intervals between measurements. Five CO₂ response curves were measured at 400 μmol m⁻² s⁻¹ PPFD and three at

Table 1. Sensitivity analysis for the calibration and calculation of *g_m* at ambient CO₂ (400 μmol mol⁻¹) and 400 μmol m⁻² s⁻¹ PPFD

All percentage increases were expressed relative to the mean for scenario 1a which used standard calibration parameters (α=0.85, β=0.5). Scenarios 1b–1e represent *g_m* values calculated using the standard calibration parameters and measured variation in *R_d* and *Γ**. Scenario 2 represents the shift in *g_m* due to measuring, and not assuming α=0.85. Scenarios 3a and 3b represent *g_m* values calculated using calibrations estimated from different plots and regression fits to light response curves. Scenario 4 represents *g_m* values calculated using variation in CO₂ to generate a linear–sigmoidal calibration curve. Values represent means and standard errors for six replicates.

Calibration type	Parameter varied	Apparent <i>g_m</i> (mol m ⁻² s ⁻¹)	% increase with calibration	
No calibration standard parameters				
1a	α=0.85, β=0.5	NA	0.166±0.018	0
1b	α=0.85, β=0.5	<i>R_d</i> +95% CI ^a	0.173±0.020	4.1
1c	α=0.85, β=0.5	<i>R_d</i> -95% CI	0.160±0.017	-3.7
1d	α=0.85, β=0.5	<i>Γ*</i> +95% CI	0.181±0.021	9.0
1e	α=0.85, β=0.5	<i>Γ*</i> -95% CI	0.154±0.016	-7.5
Measured leaf absorbance				
2	α=0.831 (measured), β=0.5	NA	0.182±0.022	9.4
Light response at 1% O ₂ and ambient CO ₂ calibration				
3a	Linear fit ^b	NA	0.341±0.087	104.5
3b	Linear–sigmoidal	NA	0.306±0.079	83.6
CO ₂ response at 1% O ₂ and 400 μmol m ⁻² s ⁻¹ light calibration				
4	Linear–sigmoidal	NA	0.199±0.017	19.8

^a *R_d* and *Γ** were estimated from six replicate sets of Laik curves: in 1b–1e the mean values were used plus or minus the 95% confidence interval of the mean for the replicates (*R_d*, 0.42±0.17 μmol m⁻² s⁻¹ and *Γ**, 36.0±1.5 μmol mol⁻¹); ^b Linear fit to high light data from the efficiency plot (Fig. 1C) for data where Φ_{co₂} is <0.05.

1000 μmol m⁻² s⁻¹ PPFD at 1% O₂. CO₂ was reduced from 400 μmol mol⁻¹ to 100 μmol mol⁻¹ in decrements of 75 μmol mol⁻¹, and after an 8 min re-acclimation at 400 μmol mol⁻¹ increasing CO₂ to 600, 800, 1000, 1500, and 2050 μmol mol⁻¹. Gas exchange was measured at each CO₂ concentration after the cuvette CO₂ concentration was stable for >120 s. A second similar series of CO₂ responses was measured after the first under 21% O₂. The leaf absorbance of 10 leaves was measured using a Taylor integrating sphere (LI-COR 1800-12).

Estimation of 'variable J' *g_m*

Values for *g_m* were estimated from the following standard formulae used in the 'variable *J*' technique (Harley *et al.*, 1992; Valentini *et al.*, 1995; von Caemmerer, 2000), and using variants of the calibrations detailed below. Mesophyll conductance to CO₂ is estimated as the ratio of the net photosynthetic rate (*A*) and the difference in CO₂ mole fraction from the intercellular airspaces (*C_i*) and the chloroplast sites of photosynthesis (*C_c*):

$$g_m = \frac{A}{C_i - C_c} \quad (1)$$

As *A* and *C_i* are provided by standard gas exchange measurements, estimation of *C_c* remains as the difficult-to-measure unknown in this equation. *C_c* is estimated assuming that Rubisco

specificity to O₂ and CO₂ ($S_{c/o}$) remains constant, and that the ratio of the carboxylation rate (V_c) to the oxygenation rate (V_o) varies in direct proportion to the concentration of CO₂ at the site of carboxylation (C_c) in the chloroplast or the concentration of oxygen (O) which is assumed not to vary. Thus:

$$C_c = \frac{V_c 2\Gamma^*}{V_o} \quad (2)$$

where Γ^* is the photo-compensation point ($=0.5 \times O/S_{c/o}$), measured using the Laisk method. V_c can be estimated as the sum of the measured A , a value for R_d assumed to be constant and equal to that measured using the Laisk method, and half of V_o :

$$V_c = A + R_d + 0.5V_o \quad (3)$$

V_o is included in V_c , as for every two oxygenations one CO₂ is released, leading to gross photosynthesis being underestimated by A . The total electron transport (J_{total}) is the sum of the reductant required for V_c , V_o , and any alternative electron transport sinks (V_{alt}). Under many conditions four electrons are used per CO₂ molecule fixed (Baker, 2008), and it is known that two photorespiratory cycles release one CO₂, thus the rate of photorespiration can be estimated by rearranging this equation:

$$V_o = J_{\text{total}}/4 - (V_c + V_{\text{alt}}) = \frac{2}{3}(J_{\text{total}}/4 - (A + R_d + V_{\text{alt}})) \quad (4)$$

Here J_{total} includes V_{alt} ; by calibration of the total electron transport rate estimated from fluorescence (J_{raw}) with measurements of $A+R_d$ under non-photorespiratory conditions—where V_{alt} and V_o are assumed to be absent—a calibrated electron transport rate (J_{cal}) can be obtained. Under photorespiratory conditions J_{cal} then represents the sum of V_c and V_o , such that:

$$V_o = J_{\text{cal}}/4 - V_c = \frac{2}{3}(J_{\text{cal}}/4 - (A + R_d)) \quad (5)$$

From a theoretical perspective C_c is relatively well defined, but see Parkhurst (1994) and Evans (2009) for issues with describing CO₂ fluxes or fluorescence with an average number representing different depths in the leaf. However, it is the practical estimation of J_{cal} and V_{alt} that remains controversial and which represents a potential source of error in the calculation of g_m . To obtain an accurate value for J_{cal} , the raw measurements of chlorophyll fluorescence (J_{raw}) must be calibrated and in doing so account for V_{alt} under the experimental conditions as follows. Fluorescence of PSII provides an initial estimate of total electron flux through the electron transport chain:

$$J_{\text{raw}} = 0.425\text{PPFD}\Phi_{\text{PSII}} \quad (6)$$

where 0.425 is the product of 0.85, the standard assumed value for leaf absorptance (α), and 0.5, the standard fraction of quanta absorbed by PSII relative to PSI (β), and Φ_{PSII} the quantum efficiency of PSII measured from fluorescence [$\Phi_{\text{PSII}}=(F_m'-F_s')/F_m'$]. If measured values for leaf absorptance are available, the assumed α , and the estimate for J_{raw} , can be improved. However the calibration procedures described below are often used to estimate a value for $\alpha\beta$ and therefore α is not typically necessary. J_{raw} then can be related to J_{A+R_d} under appropriate non-photorespiratory conditions—normally at 1% O₂—where V_o is negligible. From this relationship, the empirical values for $\alpha\beta$ can be found and thus provide a calibrated estimate of total electron flux (J_{cal}). Under non-photorespiratory conditions Equations 5 and 6 become:

$$J_{\text{cal}} = 4(A + R_d) = mJ_{\text{raw}} + c = m0.425\text{PPFD}\Phi_{\text{PSII}} + c \quad (7)$$

assuming a linear relationship. Thus the corrected value for $\alpha\beta$ is $m \times 0.425$. Alternatively, this equation is often converted from

electron transport rates to quantum efficiencies by solving for Φ_{PSII} , preferably when no intercept is present:

$$\Phi_{\text{CO}_2} = \frac{A + R_d}{\text{PPFD}} = \frac{m0.425}{4}\Phi_{\text{PSII}} = m'\Phi_{\text{PSII}} \quad (8)$$

where Φ_{CO_2} is the quantum efficiency of photosynthesis ($[A+R_d]/\text{PPFD}$), m' is the slope of the efficiency relationship, and the calibrated value for $\alpha\beta$ is $4m'$. In practice, either of these relationships (Equation 7 or 8) are used for the calibration of J_{raw} , with the fitted slopes providing an estimate of the value of $\alpha\beta$ for the calibration conditions. The intercept is usually assumed to be zero. Alternatively, the presence of a non-zero y -intercept can be tested: if present, it represents alternative electron transport at the photo-compensation point.

This calibration procedure is based upon the assumptions that: (i) α and β are constant across the range of experimental variation; (ii) it is possible to estimate alternative electron transport as a constant proportion of total electron flux estimated as the intercept of the relationship; and (iii) the non-photorespiratory measurement conditions do not alter alternative electron transport relative to the experimental conditions. If either $\alpha\beta$ or alternative electron transport vary with the environmental condition used to create the relationship (light or CO₂), non-linearities should be present in the relationship. An alternative is then to fit a non-linear function to the calibration data, such as the following linear-sigmoidal function:

$$J_{\text{cal}} = J_{A+R_d} = J_{\text{raw}} - c - a/\{1 + \exp[-(J_{\text{raw}} - b)/d]\} \quad (9)$$

Analysis of sensitivity of 'variable J' g_m magnitude to calibration scenarios

To test whether calibration variants have significant effects on the calculation of g_m , a sensitivity analysis was performed. Apparent shifts in g_m due to changing the calibrations were calculated as follows for gas exchange measurements made on six leaves under ambient conditions (400 $\mu\text{mol mol}^{-1}$ CO₂ and a PPFD of 400 $\mu\text{mol m}^{-2} \text{s}^{-1}$). (1) Standard calibration using assumed α and β values (0.85 and 0.5) as is often used for the variable J method, with the following variants: (1a) the mean R_d and Γ^* values measured using the Laisk method with six replicates; (1b) R_d plus and (1c) R_d minus the 95% CI of the mean; (1d) Γ^* plus and (1e) Γ^* minus the 95% confidence interval of the mean. (2) Standard calibration using a measured α (0.831) and assumed β value (0.5). (3) Calibrations fit to light response data measured under non-photorespiratory conditions at ambient CO₂: (3a) using a linear fit, passing through the origin on the efficiency plot, but only using data points below a Φ_{CO_2} of 0.05 as suggested by Seaton and Walker (1990) and (3b) a linear-sigmoidal fit to the combined light response data on the rate plot. (4) Calibrations fit to the CO₂ response data measured at 400 $\mu\text{mol m}^{-2} \text{s}^{-1}$ PPFD and under non-photorespiratory conditions, using the linear-sigmoidal function. Fitted parameters for the calibration functions are provided in the Results. The non-linearity of the calibrations was assessed by comparing the Akaike Information Criterion (AIC) values between linear-sigmoidal fits and linear fits, where fits with the lowest AIC values have greatest support with model complexity taken into account (Burnham and Anderson, 2004). The R statistical program was used for these analyses (R_Development_Core_Team, 2010). An apparent value for g_m was calculated for each of the six replicate leaves for all of the scenarios or parameter changes described above.

Cross-validation of 'variable J' g_m with g_m estimated from curve-fitting procedures

Values of mesophyll conductance to CO₂ were measured for an additional 10 CO₂ response curves using the same apparatus, corrections, and measurement conditions as detailed above. Added

to the five initial CO₂ response curves measured at 21% O₂, these provided a total of 15 curves, with an average of 14 CO₂ levels per curve. The measurements for the CO₂ response curves were made simultaneously with the fluorescence measurements, by using the 2 cm² LI-COR fluorescence chamber, a necessary compromise, as the goal of this experiment was cross-validation between the variable J and curve-fitting methods. Ideally, measurements for use in curve fitting should be made using larger leaf areas (Warren, 2006; Pons *et al.*, 2009).

The Exhaustive Dual Optimization (EDO) curve-fitting technique of Gu *et al.* (2010), as implemented on the LeafWeb website, was employed for this analysis in cognizance of the curve-fitting parameterization issues raised in that paper. The technique is based upon the principle that the photosynthetic CO₂ response curve can be represented by the minimum of a combination of three equations (Equation 10). These equations are non-rectangular hyperbolas that explicitly account for a non-infinite g_m , and are based upon the original Farquhar–von Caemmerer–Berry-type photosynthetic functions:

$$A = \min(A_c, A_j, A_{TPU}) \quad (10)$$

The EDO approach uses functions for these three processes approximately similar to past curve-fitting approaches (Ethier *et al.*, 2006; Warren, 2006), but applies these by assessing the possibility that any CO₂ response curve point could be limited by any of the three processes, with some constraints. The technique then exhaustively searches for parameter estimates for all of these possible limitation states, and selects the optimal fit as the fit with a minimum of a cost function consistent with the form of Equation 10. For the EDO analysis, five parameters (g_m , $V_{c,max}$, J , R_d , and the rate of triose phosphate utilization) were fit. To test for reliability of the parameter estimate for g_m , the first and second derivatives of the cost function with respect to g_m were tested to be zero and non-zero, respectively (Gu *et al.*, 2010).

To enable comparison between the two methods, g_m values for the curve-fitting procedure (representing the entire CO₂ response curve) were compared with variable J g_m values measured at ambient CO₂ (ambient CO₂ point on the CO₂ response curve), or the interpolated g_m value for a C_i of 600 $\mu\text{mol mol}^{-1}$ (interpolated as the point at a C_i of 600 $\mu\text{mol mol}^{-1}$ on the line connecting the measured g_m and C_i value greater and less than 600 $\mu\text{mol mol}^{-1}$).

Sensitivity analysis of 'variable J' g_m to CO₂ variation

The sensitivity of g_m response to variation in CO₂ to errors in the estimation of R_d or J_{cal} was assessed by introducing a constant offset into a Farquhar–von Caemmerer–Berry-type photosynthetic model that held g_m constant. A region of the modelled g_m to C_i response curve was defined from a C_i of 200–500 $\mu\text{mol mol}^{-1}$ corresponding to values for which photorespiration should not be greatly inhibited, and thus measurements of V_o would be relatively accurate. A linear slope was fit to these data, and non-zero slopes were recorded in response to introducing positive or negative biases in R_d or J_{cal} .

The photosynthetic modelling was conducted using inputs of varying C_c and constant values of g_m (0.3 mol m⁻² s⁻¹), R_d (0.42 $\mu\text{mol m}^{-2} \text{s}^{-1}$), Γ^* (36.0 $\mu\text{mol mol}^{-1}$), $V_{c,max}$ (70 $\mu\text{mol m}^{-2} \text{s}^{-1}$), and J (108 $\mu\text{mol m}^{-2} \text{s}^{-1}$). The values for these parameters were chosen to represent approximately a measured CO₂ response curve for *P. trichocarpa*. The model calculations are provided online as a spreadsheet (Supplementary Spreadsheet S1 available at JXB online). K_c and K_o values and the standard Farquhar–von Caemmerer–Berry equations were taken from von Caemmerer (2000), and reference to them is provided in the spreadsheet. From these inputs, $V_{c,min}$ was calculated from the limiting process, namely the minimum of $V_{c,c}$ and $V_{c,j}$ (the Rubisco and RuBP regeneration-limited carboxylation rates), and the photorespiration rate, V_o , calculated from $V_{c,min}$. The total RuBP regeneration rate, $J_{total}/4$, was calculated as the sum of $V_{c,min}$ and V_o , assuming no alternative electron transport sinks and strict linear

correspondence to fluorescence. Thus $J_{total}/4$ provides a value for $J_{cal}/4$, as per the variable J method. C_i was calculated using Fick's law and the calculated value for A . This model explicitly held g_m constant; a bias was then introduced into the assumed value of R_d or modelled value for $J_{cal}/4$ ($J_{total}/4$), and from these new values a 'biased' estimate of g_m was obtained using the formulae associated with the variable J method; the reverse of the initial calculations. Note that the formulae used in the variable J method given above (Equations 1–4) are algebraically the same as those used in the photosynthetic model just outlined. Thus the only difference between the biased estimate of g_m and the value for g_m when held constant is the introduction of a constant error in R_d or $J_{cal}/4$.

Results

Calibration of fluorescence estimates of electron transport rate with gas exchange

Data used to calibrate fluorescence with gas exchange can be expressed either as quantum efficiency plots or as rate plots using CO₂ or electron equivalent units. As each has its advantages, the same light or CO₂ response curve data were compared on both plots (Fig. 1). The calibration relationships relating photosynthetic rates in electron-equivalent units (J_{A+R_d}) to uncalibrated fluorescence estimates of electron transport (J_{raw}) under non-photorespiratory conditions were non-linear when measured across a broad range of light or CO₂ conditions (Fig. 1). Light response curves demonstrated three phases of non-linearity: a subtle increase in J_{raw} relative to J_{A+R_d} at low light, a large shift towards increased J_{raw} , but not J_{A+R_d} , at intermediate light, and in some responses a return to the one-to-one line at the highest light levels (Fig. 1A). For the same data plotted as efficiency plots (note the reverse in direction representing increasing light), the same shifts resulted in curvature towards greater quantum efficiency of net photosynthesis (Φ_{CO_2}) at low light (Fig. 1C). This method of plotting the same data emphasizes the second curvature towards greater PSII efficiency (Φ_{PSII}) at very low light ($\sim 100 \mu\text{mol m}^{-2} \text{s}^{-1}$).

Due to the curvature of the light response data from low to high light, two calibration relationships were fit. In the first method, a linear calibration was fit to each replicate light response on the efficiency plot forcing each line to pass through the origin (intercepts were not significantly different from the origin over this range of PPFD) and using data below a Φ_{CO_2} of 0.05 (here an average PPFD of $>500 \mu\text{mol m}^{-2} \text{s}^{-1}$), consistent with the suggestions of Seaton and Walker (1990) and resulting in $\alpha\beta=0.383$. If the calibration was done using an assumed value for α of 0.85, as is common, the calibrated β value would be 0.451 rather than 0.5. The measured value of α was 0.831, resulting in an estimate of 0.461 for the β value for higher light intensities. For comparative purposes, the one-to-one line was considered as the standard 'calibration' ($\alpha\beta=0.425$), as it is common to assume this value for $\alpha\beta$ with no further calibration. In the second calibration, a linear–sigmoidal curve was fit to all of the light response replicates simultaneously for the rate plot (Equation 9, a linear–sigmoidal fit: $a=11.1$, $b=99.9$, $c=1.87$, $d=8.31$, adjusted $R^2=0.974$, AIC value=597.47). A linear fit

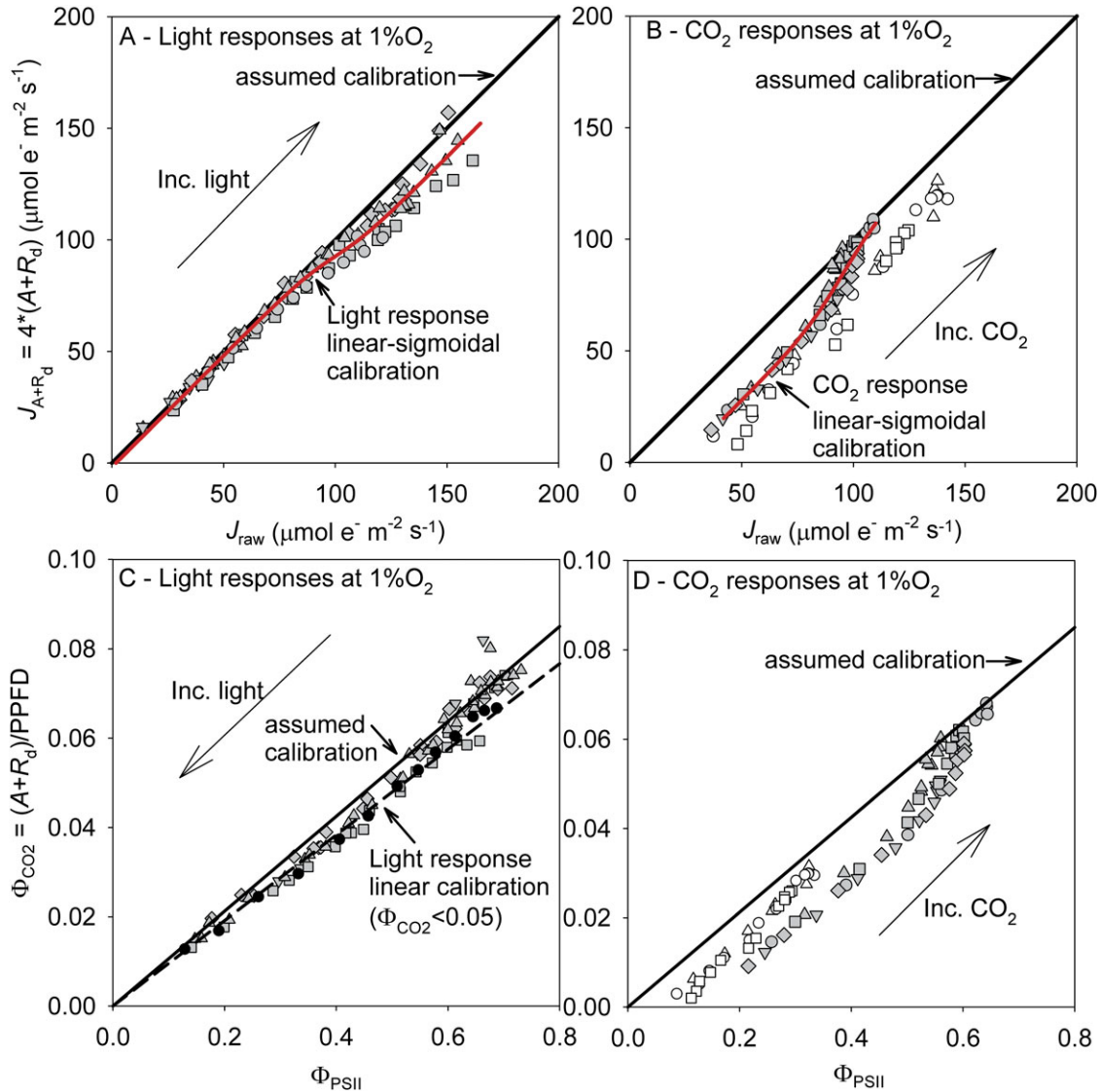


Fig. 1. Calibration plots for the rate of photosynthesis versus electron transport estimated from fluorescence (A and B), or for the photosynthetic versus fluorescence quantum efficiencies (C and D), measured under non-photorespiratory conditions (1% O_2) using light response curves (A and C) or CO_2 response curves with $400 \mu mol m^{-2} s^{-1}$ or $1000 \mu mol m^{-2} s^{-1}$ PPFD (grey and white symbols) (B and D). J_{raw} was calculated using standard parameters ($J_{raw} = \alpha\beta \times PPFD \times \Phi_{PSII}$, $\alpha=0.85$, $\beta=0.5$, thus $\alpha\beta=0.425$). Three lines are shown: the line where $J_{cal}=J_{raw}$ (solid line; all panels), the average linear fit for nine light responses on the efficiency plot for points below a Φ_{CO_2} of 0.05 (dashed line; C) and the average fitted linear-sigmoidal curve fit to the data of the nine light or five CO_2 responses (A and B). Different symbols represent measurements on different leaves. In C, one representative response curve is highlighted in black to illustrate regions of concave curvature at low Φ_{CO_2} s and a final increase in Φ_{PSII} at high Φ_{CO_2} (low light). Arrows demonstrate the direction in which light or CO_2 increases on the different calibration plots.

to the same data resulted in a marginally higher AIC value (598.81) and similar adjusted R^2 (0.974).

It is common to use light response curves to calibrate the variable J method and then make use of them in studies using other experimental stimuli, for example variation in CO_2 . The carbon dioxide response curves measured at low O_2 and $400 \mu mol m^{-2} s^{-1}$ PPFD did not resemble the light response curves at lower CO_2 concentrations, or at higher light (Fig. 1B). A large shift was observed in the opposite direction to the light response curves, consistent with an increase in alternative electron sinks as may be expected by the lack of photosynthetic ability to use reductant under

conditions of high light, low CO_2 , and low O_2 . As the high CO_2 points were measured after the low CO_2 points, and showed high efficiency nearing the one-to-one line, photo-inhibition was not apparent (also F_v'/F_m' returned to pre-low CO_2 exposure levels). The relationship on the efficiency plot was not linear; therefore, the CO_2 response curves were only calibrated using a linear-sigmoidal function on the rate plots (Equation 9, a linear-sigmoidal fit: $a=22.8$, $b=95.3$, $c=-0.51$, $d=-8.6$, adjusted $R^2=0.958$, AIC value=357.7). A linear fit to the same data resulted in a considerably higher AIC value (367.6) and lower adjusted R^2 (0.949), the difference between AIC values of ~ 10 signifying that the

linear–sigmoidal fit had more support than the linear fit, despite taking into account the extra parameters in the linear–sigmoidal model (Burnham and Anderson, 2004). At a higher PPFd of 1000 $\mu\text{mol m}^{-2} \text{s}^{-1}$, CO₂ responses showed greater deviation from the one-to-one line, with $\sim 40 \mu\text{mol e}^{-} \text{m}^{-2} \text{s}^{-1}$ of apparent electron transport for little assimilation at the lowest CO₂ levels. To the authors' knowledge, robust data have not been presented to validate that the calibration relationship is the same between conditions of varying light and CO₂, apart from Hassiotou *et al.* (2009) whose results largely confirm those in Fig. 1. Most studies use a single saturating flash to measure F_m' , potentially introducing additional non-linear effects with changing light (Markgraf and Berry, 1990; Earl and Ennahli, 2004). However, measurements of varying light demonstrated that using multiple saturating flashes rather than a single flash did not linearize the calibration functions, and rather the size of the discrepancy between J_{A+R_d} and J_{raw} was slightly enhanced at high PPFds (F_m' increases while F_s remains constant). As the key CO₂ calibrations were done at moderate PPFd (400 $\mu\text{mol m}^{-2} \text{s}^{-1}$), these were not affected.

Size of calibration biases on J_{cal} and g_m

From the data shown in Fig. 1, five types of calibrations were performed: the three linear or linear–sigmoidal functions, the standard assumed calibration parameters from the literature, and the measured leaf absorbance and assumed β . The magnitude of the errors in J_{cal} on the rate plots, and particularly the efficiency plots, is both difficult to visualize and hard to relate to the magnitude of the measured quantities. Therefore, data were expressed as the residuals for the rate relationship, rescaled to units of CO₂ uptake, and plotted against the PPFd or CO₂ used to generate the points (Fig. 2A, B). The residuals were calculated as $J_{\text{cal}}/4 - A$, where J_{cal} is the electron transport rate calibrated using one of the five types of calibration.

The linear–sigmoidal calibrations applied to the same environmental variation to which they were fit produced the smallest residuals, and did not have any systematic errors across a broad range of light or CO₂, possibly apart from 2000 $\mu\text{mol m}^{-2} \text{s}^{-1}$ PPFd (Fig. 2A). The linear higher light calibration produced few residuals at high light, but consistently underestimated A by $\sim 1 \mu\text{mol CO}_2 \text{m}^{-2} \text{s}^{-1}$ at low light. The standard calibration, assuming $\alpha\beta=0.425$, performed poorly, with significant overestimates of A of up to 4 $\mu\text{mol CO}_2 \text{m}^{-2} \text{s}^{-1}$ under all but low light conditions. The standard calibration was even worse for low CO₂ conditions (Fig. 2B), resulting in residuals as high as 6 $\mu\text{mol CO}_2 \text{m}^{-2} \text{s}^{-1}$. The calibration with assumed value for β and measured α had a similar pattern to the standard calibration although the residuals were improved.

The variation between these calibration curves resulted in large differences in apparent g_m values when applied to measured photosynthetic data for ambient CO₂ and moderate light (Table 1). Values ranged by 104% from a minimum of the standard assumed calibration to that of the linear calibration. Linear–sigmoidal fits to light or CO₂ response

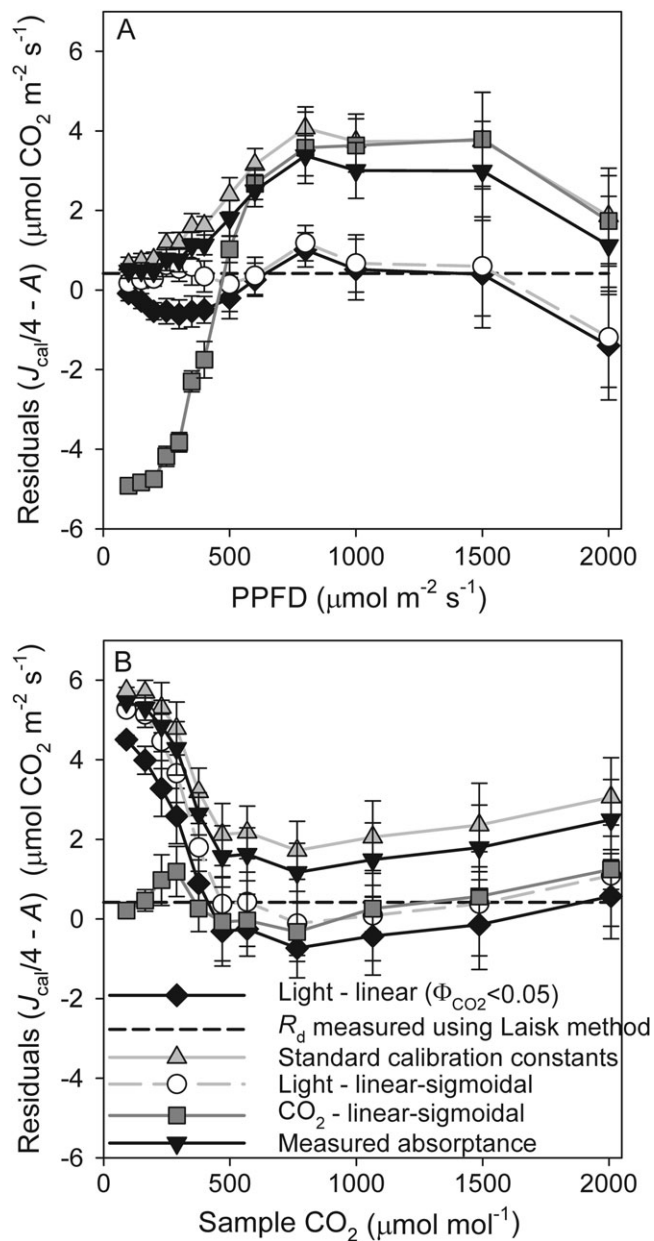


Fig. 2. The average residuals of the calibrated rate of electron transport (J_{cal}), rescaled to units of CO₂ uptake, relative to the observed photosynthetic rate for light (A) or CO₂ response curves (B) measured under non-photorespiratory conditions. To allow for possible trends in R_d , residuals were calculated as $J_{\text{cal}}/4 - A$. Points represent the mean and standard errors for five or more replicate light curves (the same data as in Fig. 1A and C) or five CO₂ response curves (the same data as in Fig. 1B and D).

curves were intermediate. This variation in apparent g_m due to the underlying calibration was larger than variation in g_m caused by changes in R_d or Γ^* when adjusted by the 95% CIs of the mean values (Table 1).

Correspondence between 'variable J' g_m and curve-fitting g_m

The g_m values calculated by the variable J and EDO approach curve-fitting method were most highly correlated,

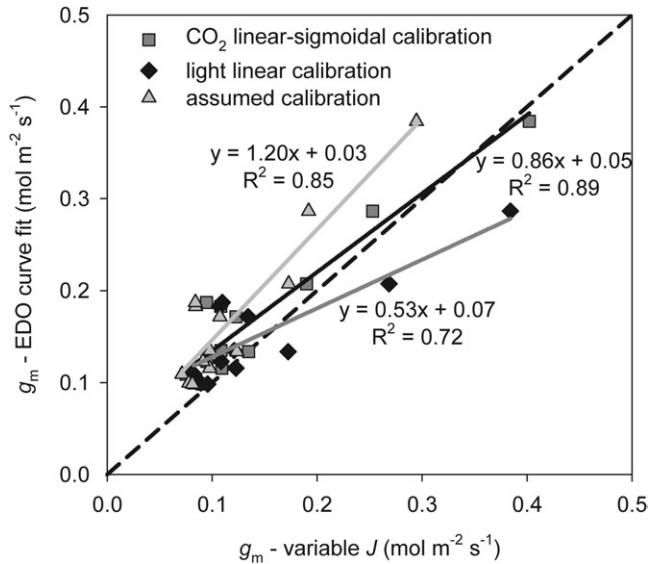


Fig. 3. Cross-validation of g_m values calculated from 15 CO_2 response curves using three alternative calibrations for the variable J method and applied to the ambient CO_2 measurement on the curve, and g_m calculated from the Exhaustive Dual Optimization (EDO) approach for fitting Farquhar–von Caemmerer–Berry models of Gu *et al.* (2010). Experimental conditions were: PPFD, $400 \mu\text{mol m}^{-2} \text{s}^{-1}$; T_l , $24.9 \pm 0.8 \text{ }^\circ\text{C}$; VPD, $1.47 \pm 0.49 \text{ kPa}$.

and the points nearest the one-to-one line for the CO_2 linear–sigmoidal calibration (Fig. 3). The assumed and linear-light calibrations resulted in correlations between the variable J g_m and the curve-fitting g_m values, but resulted in greater deviation from the one-to-one relationship. In addition, the linear-light calibration resulted in a negative value of g_m , which was removed from the analysis. Two g_m values were removed from all analyses due to the EDO curve-fitting analysis providing high g_m values ($>0.5 \text{ mol m}^{-2} \text{ s}^{-1}$), and this was consistent with a zero second derivative of the EDO cost function (the condition under which the parameter estimate is not reliable). For this analysis the variable J g_m estimate was limited to measurements made at ambient CO_2 , while the curve-fitting estimate used the entire CO_2 response curve data. When the variable J g_m value representing a C_i of $600 \mu\text{mol mol}^{-1}$ was plotted against the curve-fit g_m value, R^2 s were reduced and the variable J g_m value was an underestimate for all calibrations. For the linear-light calibration a number of variable J g_m estimates at high C_i were negative.

Response of g_m to CO_2

The response of g_m to CO_2 (detrended for stomatal conductance changes by using C_i) was highly variable when the five calibration protocols were compared (Fig. 4). In one of the five replicates (Fig. 4A), all five calibrations produced values for g_m in the range of past reports (Niinemets *et al.*, 2009); in the other four replicates the linear and linear–sigmoidal fit to the light response calibration resulted in negative or large (>1) values for g_m at CO_2 levels higher than ambient (one representative replicate is shown in Fig. 4B).

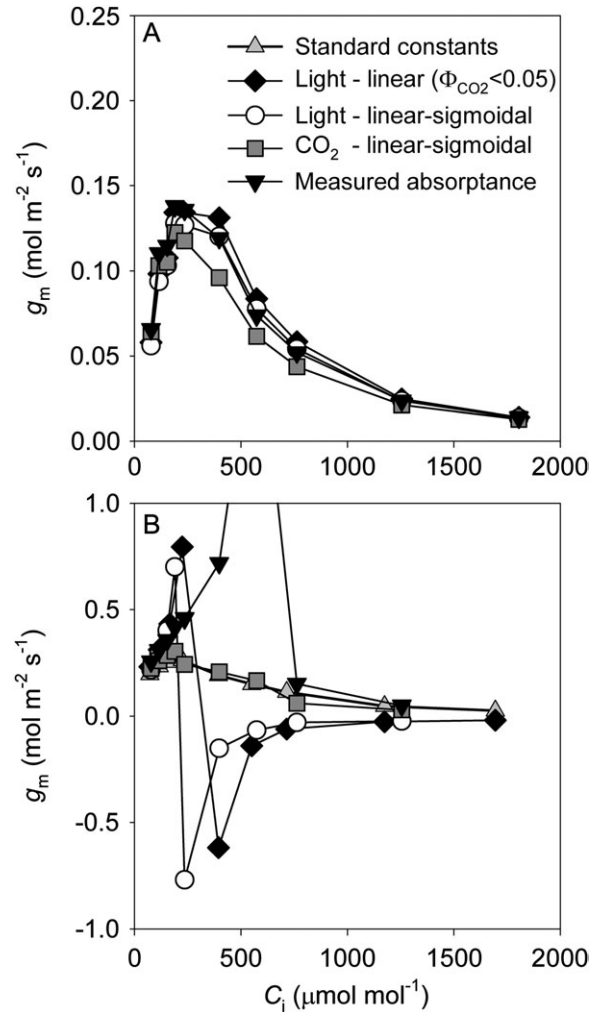


Fig. 4. The observed response of g_m to C_i illustrating either qualitative agreement amongst the four calibration options (representative of only one of five replicate CO_2 response curves; A) or marked disagreement between calibration methods (a representative CO_2 response curve for four of five replicates; B). Note that in B two of the calibration options result in negative values of g_m due to overestimates of C_c (apparent $C_c > C_i$). These occur as $g_m = A / (C_i - C_c)$, thus underestimates of J_{cal} at high C_i due to the different calibrations lead to C_c approaching C_i , the denominator of the equation is small leading to g_m approaching infinity, and when C_c becomes higher than C_i , g_m instantly becomes negative. Experimental conditions were the same as in Fig. 3.

As only the standard calibration constants and the linear–sigmoidal fit to the CO_2 response calibration gave reasonable values for g_m for all replicates, these two calibration protocols were investigated in greater detail. Using either calibration, g_m showed strong shifts, increasing from the lowest C_i values, remaining stable or slowly decreasing at ambient CO_2 values, and decreasing strongly at high C_i s (Fig. 5A, B). However, the Harley *et al.* (1992) criterion was violated for almost all points at high C_i . Nevertheless, the points that satisfy the Harley criterion (Harley *et al.*, 1992) demonstrate a consistent negative response of g_m to C_i .

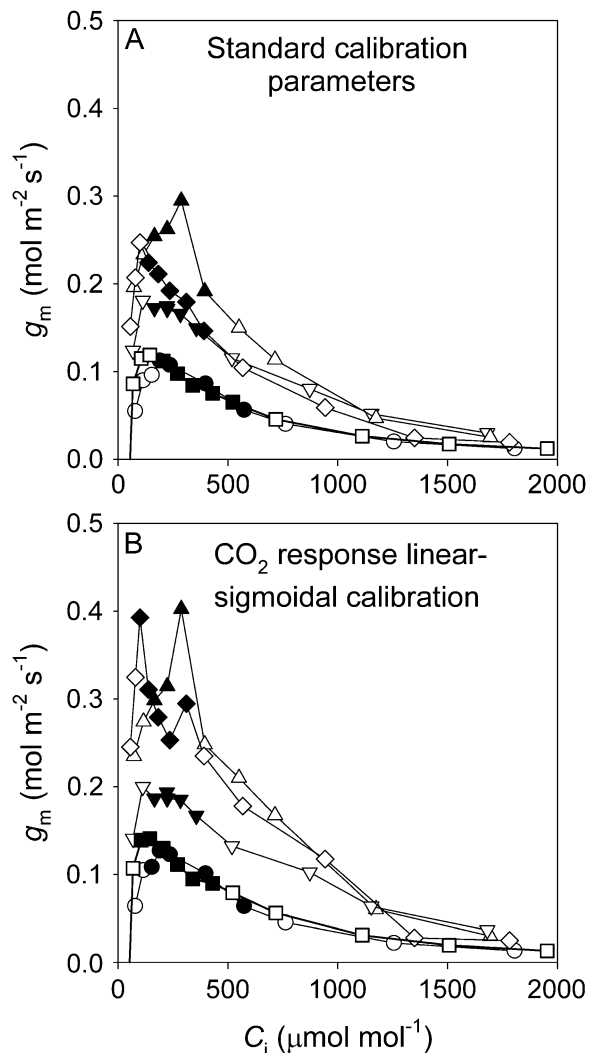


Fig. 5. Observed g_m response to C_i for five replicate CO₂ response curve using the standard calibration constants (A) and the linear–sigmoidal fit to the CO₂ response calibration (B). Points that satisfy the Harley criterion (filled symbols) and points that had a Harley criterion of <10 or >50 (open symbols) are distinguished. Replicate curves are shown with the same symbols. Experimental conditions were the same as in Fig. 3.

The potential for calibration biases to affect the calculation of g_m can be illustrated by plotting C_i versus the parameters used to estimate C_c and g_m (Fig. 6). As C_i increases, V_o tends towards zero due to competitive inhibition of photorespiration by CO₂. As a result, C_c —proportional to the V_c/V_o ratio—is increasingly vulnerable to biases at high C_i . Specifically, as V_o decreases at higher CO₂s, any errors in its estimation lead to an inflated C_c (calculated from the V_c/V_o ratio), as C_c tends towards C_i , g_m values [calculated from $A/(C_i - C_c)$] rapidly become large. Once C_c , estimated with slight errors, is the same or larger than C_i , g_m becomes infinite or negative. This explains the variability, high and negative values of g_m in Fig. 4. Furthermore, as V_o tends towards zero, biases in $J_{\text{cal}}/4$ due to alternative electron transport sinks (or changes in R_d , α , or β) become increasingly important. In other words, small

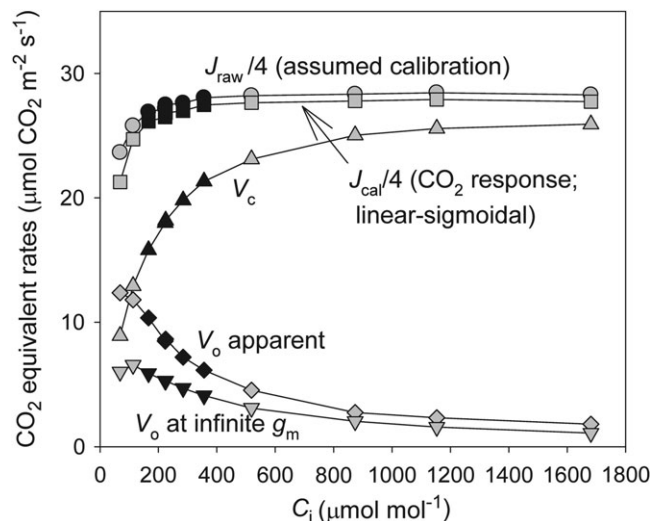


Fig. 6. Rates of the standard fluorescence estimate of electron transport (J_{raw}), the calibrated rate of electron transport expressed in CO₂ equivalents, carboxylation (V_c), apparent photorespiration rate (V_o apparent = $J_{\text{cal}}/4 - V_c$), and photorespiration calculated assuming $C_c = C_i$ (V_o at infinite g_m), for a measured response to CO₂. Note the small shift in V_o necessary to result in an infinite g_m at high CO₂. Points that satisfy the Harley criterion (filled symbols) and those that did not (open symbols) are distinguished. Experimental conditions were the same as in Fig. 3.

errors in the estimation of J_{cal} have increasing impact on the estimation of g_m at high C_i , as V_o becomes small and the error to the V_o ratio increases.

Sensitivity of response of g_m to CO₂

The sensitivity of g_m to calibration biases was further investigated by introducing small biases in $J_{\text{cal}}/4$ into a photosynthetic model. The lines in Fig. 7A represent the apparent g_m response for simulated data for which g_m was held constant, but for which small systematic errors were introduced into the value for $J_{\text{cal}}/4$ and g_m then calculated from the biased data. Any overestimation of $J_{\text{cal}}/4$ results in a lower g_m and an apparent negative relationship with increasing C_i (Fig. 7A). In contrast, underestimating $J_{\text{cal}}/4$ results in a larger apparent g_m . The presence of a positive or negative relationship between g_m and C_i was a function of the small constant biases added to $J_{\text{cal}}/4$ (Fig. 7B). If, in the photosynthetic model, g_m is assumed to be constant with CO₂, then the residuals in Fig. 7B demonstrate that previously used calibration relationships would consistently result in apparent negative g_m responses to CO₂, while the linear–sigmoidal CO₂ response calibration would result in both negative and positive relationships. If this assumption is true, the sensitivity analysis demonstrates that the bias in $J_{\text{cal}}/4$ necessary to result in an artefactual effect of C_i on g_m is small (<0.5 $\mu\text{mol CO}_2 \text{ m}^{-2} \text{ s}^{-1}$) relative to the residuals typically observed in the calibration relationship (~0.5–6 $\mu\text{mol CO}_2 \text{ m}^{-2} \text{ s}^{-1}$; Fig. 2A or B and Fig. 7B). If, however, g_m is truly not constant, the observed slope of the response of g_m to CO₂ would still be sensitive to errors, and

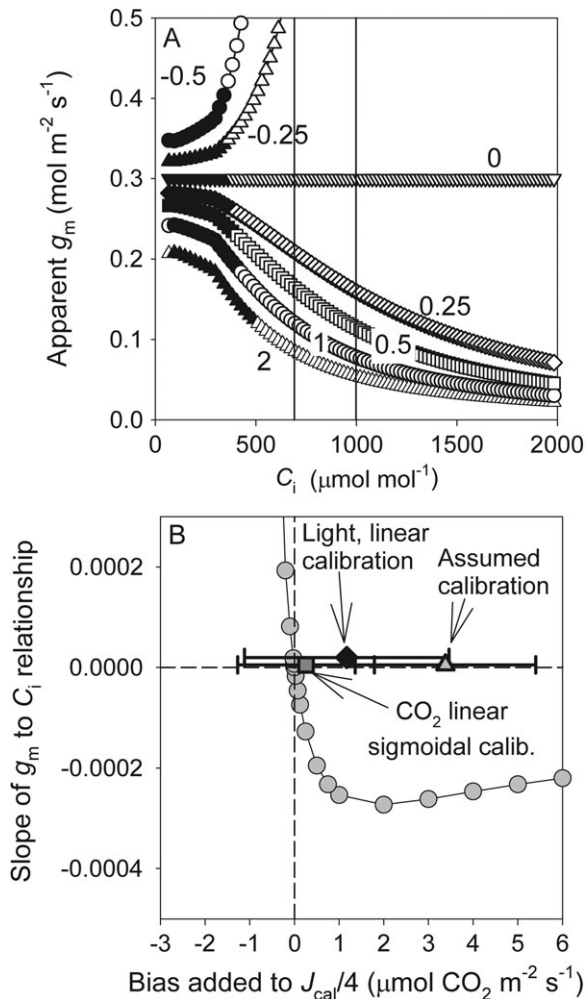


Fig. 7. The sensitivity of the g_m to C_i response to constant errors added to $J_{\text{cal}}/4$ for a photosynthesis model that had a constant g_m (A) and the sensitivity of the slope of the g_m to C_i response for the same errors in the photosynthesis model (B). Average and standard deviations of the residuals [$J_{\text{cal}}/4 - (A + R_d)$] of three calibration options are shown in B. The slope of the g_m to C_i response was defined as the linear fit to the modelled data within a range of C_i s that would satisfy the criterion of Harley *et al.* (1992) (200–500 $\mu\text{mol mol}^{-1}$). The residuals were calculated across the same range of C_i . Numbers in A represent the overestimate (error) added to $J_{\text{cal}}/4$ where zero error (and thus the true modelled relationship) had no relationship between g_m and C_i . Vertical lines in A represent the C_i at which g_m estimates shifted from high to negative values (see text for explanation).

if errors were large enough would result in transitions from negative to positive or vice versa. The model is included as a spreadsheet in the Supplementary data at JXB online.

Discussion

Can the variable J method measure the response of g_m to CO_2 ?

The nature of the observed response of g_m to CO_2 is highly sensitive to biases in the estimation of the calibrated total

photosynthetic electron transport rate (J_{cal}). This was demonstrated using a sensitivity analysis of standard photosynthetic equations, to which a systematic bias was added. For example, the sensitivity is such that there is an apparent 23% decrease in g_m over a 300 $\mu\text{mol mol}^{-1}$ range of C_i when an $\sim 2\%$ ($\sim 0.5 \mu\text{mol CO}_2 \text{m}^{-2} \text{s}^{-1}$) overestimate of $J_{\text{cal}}/4$ is included in the photosynthetic model, despite the modelled g_m remaining constant (Fig. 7A). As the true modelled relationship was on the steepest portion of the sensitivity analysis (Fig. 7B), this demonstrates that if g_m is indeed constant, then any bias in $J_{\text{cal}}/4$ will lead to artefactual positive or negative relationships of g_m to C_i . If g_m is dynamic, varying with CO_2 , the point of greatest sensitivity will drift, but the overall pattern of sensitivity demonstrated will remain. In this case, an observed relationship may represent a true response, but the slope will be sensitive to measurement errors and calibration biases. This sensitivity analysis provides similar results to those which Harley *et al.* (1992) presented in their fig. 6, and those which Hassiotou *et al.* (2009) presented in their supplementary material. Indeed, Harley *et al.* (1992) note that: ‘In all cases, the sensitivity to errors was relatively low between 100 and 300 $\mu\text{bar } C_i$, but outside this range the sensitivity was so great that the results could become unreliable.’ Despite these earlier cautions, subsequent researchers have continued to use this approach over a broad range of conditions. It is important to note that these considerations are applicable to any environmental variation that may affect photorespiration: CO_2 , temperature, light, stomatal closure, etc. For instance, a similar analysis could be done for the relationship of g_m to PPFD, in which case the relationship would be sensitive to errors at PPFDs below light saturation where the errors become significant relative to photorespiration. Thus it is also the relationship of g_m to light that is sensitive to errors when using the variable J method, although at saturating light intensities the presence of high rates of photorespiration leads to less sensitive estimates of the relationship of g_m to light.

The residual variation in the different calibration relationships—which is a determinant of the error in $J_{\text{cal}}/4$ —was up to 5 $\mu\text{mol CO}_2 \text{m}^{-2} \text{s}^{-1}$ at the extreme of using standard calibration constants, and about $\pm 1 \mu\text{mol CO}_2 \text{m}^{-2} \text{s}^{-1}$ when calibrated using a linear–sigmoidal function on CO_2 response data (Fig. 2A, B). Thus, the magnitude of the errors in the calibrations was similar to, or considerably larger than, the error necessary to affect whether there is an apparent response of g_m to C_i (Fig. 7B). It is broadly true then, given the large errors in our best estimates of $J_{\text{cal}}/4$, and the sensitivity of the g_m to C_i relationship to any error, that it is difficult to measure the response of g_m to C_i using the variable J method. That is, with the high overestimates of J_{cal} demonstrated for standard calibration methods over a moderate CO_2 range (Fig. 7B), the variable J method is likely to produce steeper relationships between g_m and CO_2 than actually exist.

Variable J g_m and partially independent g_m values from the EDO curve-fitting approach corresponded well when the variable J technique was limited to use under ambient

CO₂ and with the non-linear calibrations reported here (Fig. 3). These results are consistent with the sensitivity analysis performed earlier (Table 1). That is, relative to the EDO curve-fitting g_m values the linear-light calibration causes overestimates in variable J g_m , the CO₂ linear-sigmoidal calibration results in approximate correspondence, and the assumed calibration results in underestimates. This suggests that when appropriately calibrated the variable J method has value for studies comparing species, using unstressed plants at moderate light and ambient CO₂, but should not be applied across a range of environmental conditions under which photorespiration is likely to vary. However, these non-linear calibrations remain empirical and do not address the implication that a non-linear response represents an unaccounted for fundamental change in photosynthetic functioning.

Why are the calibrations non-linear?

It is difficult to provide a retrospective review of whether the non-linearities in the calibration relationships observed here are present in the g_m literature. For example, a literature review of 56 experimental studies of g_m , published since 1992, found that 66% of these use the variable J method, and 44% use it as a sole technique. Of these, few studies provided calibration data, and if this was done even fewer calibrated the variable J method using environmental variation appropriate for the experiment at hand. Fewer performed brief sensitivity analyses, and finally no study attempted to calibrate the technique using non-linear functions. However, many of the non-linear effects described here have been previously described by Seaton and Walker (1990) and Oquist and Chow (1992). There are also indications of non-linearities in the calibration relationships used to calculate g_m or C_c (Warren, 2006; Galle *et al.*, 2009; Hassiotou *et al.*, 2009; Loreto *et al.*, 2009).

Seaton and Walker (1990) and Oquist and Chow (1992) demonstrated large non-linearities in light response curves, plotted as efficiency plots, measured under non-photorespiratory, saturating CO₂ conditions and with oxygen electrodes. These curved relationships on efficiency plots are consistent with the sigmoidal patterns found on the rate plots, but there are clear differences in weighting of points between the plots. The reasons for the non-linearities are discussed by Oquist and Chow (1992) and include: (i) changing connectivity of PSII units, leading to more cycling of electrons between chlorophylls; (ii) at low light, mitochondrial respiration (R_d) may increase, but in the variable J calculations R_d is assumed to be constant and a single value usually estimated for all conditions from Laik response curves; (iii) fluorescence parameters may be estimated from slightly shallower populations of chloroplasts than those that fix CO₂, and the contributions of these populations of chloroplasts would change with light intensity (Warren, 2006; Evans, 2009). On the rate plots, possible alternative electron sinks are highlighted, resulting in non-linear shifts in the calibration relationship, and may represent little (Ruuska *et al.*, 2000), or up to 24% of the

total electron flux (Haupt-Herting and Fock, 2002). Two main processes are thought to account for alternative electron sinks (von Caemmerer, 2000), each accounting for up to 10% of total electron flux: reductant provided to nitrate assimilation (Rachmilevitch *et al.*, 2004) and the Mehler reaction (Haupt-Herting and Fock, 2002).

These effects are highlighted when comparing light and CO₂ responses measured under non-photorespiratory conditions (Fig. 1A, B). *A priori* this must be expected, as at low CO₂, and particularly at high light, there is a limitation on reductant use, but high reductant supply that will result in large alterations of PSII heat dissipation and may result in up-regulation of alternative dissipative energy sinks, such as the Mehler reaction (Neubauer and Yamamoto, 1992). The quantitative effects of alternative energy sinks remain unclear (Ruuska *et al.*, 2000); however, it is noted that relative to the errors ($\sim 2\%$ of $J_{\text{total}}/4$) necessary to cause apparent changes in g_m , estimates of alternative electron sinks are large and therefore vital to account for.

Finally, it is not clear whether alternative electron sinks are changed when shifting from ambient to low O₂ as required for the calibration curves (Pons *et al.*, 2009). For instance, at high CO₂ the calibration curve was closer to the one-to-one line than for high light points (Fig. 1). This may imply that alternative electron transport sinks are affected by the capacity of photosynthesis to dissipate absorbed light energy, or are directly affected by CO₂. Considerable shifts in nitrate assimilation with age, CO₂, and oxygen concentration occur in *Arabidopsis*, using an equivalent electron flux up to 10% of the photosynthetic rate (Rachmilevitch *et al.*, 2004), and thus represent evidence of alternative electron transport shifts that could occur during the calibration procedure. If this is generally the case, it would be challenging to find conditions under which the variable J method can be calibrated. Indeed, the fitted α or β parameters for a non-linear calibration function cannot then be interpreted as physical constants as the non-linearity implies that they change with environmental conditions, or that they include alternative electron transport sinks. It appears that much work remains to be done, using independent methods, to understand the implications of the photosynthetic changes that occur when producing calibration relationships for the estimation of g_m and C_c using the variable J method.

How should the variable J method be used?

The variable J method appears difficult to validate under circumstances of varying photorespiration due to the extreme sensitivity of g_m under conditions of low photorespiration. However, the method when calibrated taking non-linearities into account did improve the estimates of g_m under ambient CO₂ relative to the EDO curve-fitting approach. Thus if the variable J method is to be used for comparing species (and not environmental variation) the following are imperative: (i) a calibration is done with conditions that match the experimental conditions (not a light calibration versus CO₂ experiment); (ii) the

calibration (and experiment) is limited to the linear region, for example $\Phi_{CO_2} < 0.05$; Seaton and Walker (1990), or non-linear functions are used, and if not linearity should be explicitly tested; (iii) the calibration is fit using rate plots, not the efficiency plots that emphasize low photosynthetic rate points disproportionately; and (iv) a sensitivity analysis is done that asks what size biases in the estimation of J_{cal} , or variation in the values for R_d and Γ^* , are necessary to remove the observed effect or relationship, and are such errors plausible for the calibrations. Regardless of these improvements, the lack of knowledge of why the calibration response is curved, and whether alternative electron sinks are affected by changing O_2 may preclude the use of the variable J method in most experiments.

Conclusion

The variable J method is sensitive to errors and must be used with caution in experiments where photorespiration varies. Nevertheless, none of the calibration or sensitivity scenarios tested here precludes an effect of any variable on g_m ; thus g_m may be dynamic rather than constitutive, but these results suggest that we cannot know the magnitude or nature of changes with certainty using this technique. It is suggested to limit use of the variable J method to comparing species under conditions of moderate light and ambient CO_2 with appropriate calibration, and not in experiments measuring responses to environmental factors that affect photorespiration. There is much research needed using independent methods to provide information on whether and how g_m and alternative electron sinks respond to CO_2 , light, or O_2 . The region at which g_m measured using the variable J method starts declining with CO_2 (Flexas *et al.*, 2007) or reduced light (personal observation) corresponds to the point where RuBP regeneration becomes limiting to photosynthesis. Although this may occur through a common mechanism related to RuBP regeneration, this effect is less apparent in g_m measurements using carbon isotope discrimination (Flexas *et al.*, 2007; Tazoe *et al.*, 2009, 2011; Vrabl *et al.*, 2009). The point where RuBP regeneration becomes limiting for both the light and CO_2 response curves also corresponds to a decrease in photorespiration. Thus at this point the ratio of biases to photorespiration dramatically increases, causing artefacts to be introduced into the response of variable J g_m to CO_2 or light, if subtle biases are present in the calibration or measurements. Thus, it is suggested that positive biases in the calibration procedure result in the variable J method overestimating the slope of the relationship between g_m and C_i —an explanation for the differences between studies using the variable J method and those using carbon dioxide discrimination.

Supplementary data

Supplementary data are available at *JXB* online.

Spreadsheet S1. Sensitivity analysis of modelled photosynthetic response to CO_2 , with g_m held constant.

Acknowledgements

This research was funded in part by USDA-CREES grant number 2006-35100-7263, a Spanish Ministry of Education and Research project AGL2005-06927-CO2-01/AGR (to AP), and a Giorgio Ruffolo Fellowship in the Sustainability Science Program at Harvard University (to MG) for which the Italian Ministry for Land, Environment and Sea is gratefully acknowledged. We thank Jessica Savage for comments on the manuscript, and Lianhong Gu and the creators of the EDO curve-fitting website at <http://www.leafweb.ornl.gov>.

References

- Anon. 2004. *Using the LI-6400 portable photosynthesis system*. Lincoln, NE: LI-COR Biosciences.
- Baker NR. 2008. Chlorophyll fluorescence: a probe of photosynthesis *in vivo*. *Annual Review of Plant Biology* **59**, 89–113.
- Burnham KP, Anderson DR. 2004. Multimodel inference—understanding AIC and BIC in model selection. *Sociological Methods and Research* **33**, 261–304.
- Earl HJ, Ennahli S. 2004. Estimating photosynthetic electron transport via chlorophyll fluorometry without Photosystem II light saturation. *Photosynthesis Research* **82**, 177–186.
- Ethier GJ, Livingston NJ, Harrison DL, Black TA, Moran JA. 2006. Low stomatal and internal conductance to CO_2 versus Rubisco deactivation as determinants of the photosynthetic decline of ageing evergreen leaves. *Plant, Cell and Environment* **29**, 2168–2184.
- Evans JR. 2009. Potential errors in electron transport rates calculated from chlorophyll fluorescence as revealed by a multilayer leaf model. *Plant and Cell Physiology* **50**, 698–706.
- Flexas J, Diaz-Espejo A, Galmes J, Kaldenhoff R, Medrano H, Ribas-Carbo M. 2007. Rapid variations of mesophyll conductance in response to changes in CO_2 concentration around leaves. *Plant, Cell and Environment* **30**, 1284–1298.
- Galle A, Florez-Sarasa I, Tomas M, Pou A, Medrano H, Ribas-Carbo M, Flexas J. 2009. The role of mesophyll conductance during water stress and recovery in tobacco (*Nicotiana sylvestris*): acclimation or limitation? *Journal of Experimental Botany* **60**, 2379–2390.
- Genty B, Briantais JM, Baker NR. 1989. The relationship between the quantum yield of photosynthetic electron-transport and quenching of chlorophyll fluorescence. *Biochimica et Biophysica Acta* **990**, 87–92.
- Gu LH, Pallardy SG, Tu K, Law BE, Wullschlegel SD. 2010. Reliable estimation of biochemical parameters from C_3 leaf photosynthesis–intercellular carbon dioxide response curves. *Plant, Cell and Environment* **33**, 1852–1874.
- Harley PC, Loreto F, Di Marco G, Sharkey TD. 1992. Theoretical considerations when estimating the mesophyll conductance to CO_2

flux by analysis of the response of photosynthesis to CO₂. *Plant Physiology* **98**, 1429–1436.

Hassiotou F, Ludwig M, Renton M, Veneklaas EJ, Evans JR.

2009. Influence of leaf dry mass per area, CO₂, and irradiance on mesophyll conductance in sclerophylls. *Journal of Experimental Botany* **60**, 2303–2314.

Haupt-Herting S, Fock HP. 2002. Oxygen exchange in relation to carbon assimilation in water-stressed leaves during photosynthesis. *Annals of Botany* **89**, 851–859.

Lawlor DW, Tezara W. 2009. Causes of decreased photosynthetic rate and metabolic capacity in water-deficient leaf cells: a critical evaluation of mechanisms and integration of processes. *Annals of Botany* **103**, 561–579.

Loreto F, Tsonev T, Centritto M. 2009. The impact of blue light on leaf mesophyll conductance. *Journal of Experimental Botany* **60**, 2283–2290.

Markgraf T, Berry J. 1990. Measurement of photochemical and non-photochemical quenching: correction for turnover of PS2 during steady-state photosynthesis. In: Baltscheffsky M, ed. *Current research in photosynthesis*, Vol. IV. Dordrecht, The Netherlands: Kluwer Academic Publishers, 279–282.

Neubauer C, Yamamoto HY. 1992. Mehler-peroxidase reaction mediates zeaxanthin formation and zeaxanthin-related fluorescence quenching in intact chloroplasts. *Plant Physiology* **99**, 1354–1361.

Niinemets U, Diaz-Espejo A, Flexas J, Galmes J, Warren CR.

2009. Role of mesophyll diffusion conductance in constraining potential photosynthetic productivity in the field. *Journal of Experimental Botany* **60**, 2249–2270.

Oquist G, Chow WS. 1992. On the relationship between the quantum yield of photosystem-II electron-transport, as determined by chlorophyll fluorescence and the quantum yield of CO₂-dependent O₂ evolution. *Photosynthesis Research* **33**, 51–62.

Parkhurst DF. 1994. Diffusion of CO₂ and other gases inside leaves. *New Phytologist* **126**, 449–479.

Pons TL, Flexas J, von Caemmerer S, Evans JR, Genty B,

Ribas-Carbo M, Brugnoli E. 2009. Estimating mesophyll conductance to CO₂: methodology, potential errors, and recommendations. *Journal of Experimental Botany* **60**, 2217–2234.

R_Development_Core_Team. 2010. *R: a language and environment for statistical computing*. Vienna: R Foundation for Statistical Computing.

Rachmilevitch S, Cousins AB, Bloom AJ. 2004. Nitrate assimilation in plant shoots depends on photorespiration. *Proceedings of the National Academy of Sciences, USA* **101**, 11506–11510.

Ruuska SA, Badger MR, Andrews TJ, von Caemmerer S. 2000. Photosynthetic electron sinks in transgenic tobacco with reduced amounts of Rubisco: little evidence for significant Mehler reaction. *Journal of Experimental Botany* **51**, 357–368.

Seaton GGR, Walker DA. 1990. Chlorophyll fluorescence as a measure of photosynthetic carbon assimilation. *Proceedings of the Royal Society B: Biological Sciences* **242**, 29–35.

Sharkey TD, Bernacchi CJ, Farquhar GD, Singaas EL. 2007. Fitting photosynthetic carbon dioxide response curves for C₃ leaves. *Plant, Cell and Environment* **30**, 1035–1040.

Tazoe Y, von Caemmerer S, Badger MR, Evans JR. 2009. Light and CO₂ do not affect the mesophyll conductance to CO₂ diffusion in wheat leaves. *Journal of Experimental Botany* **60**, 2291–2301.

Tazoe Y, Von Caemmerer S, Estavillo GM, Evans JR. 2011. Using tunable diode laser spectroscopy to measure carbon isotope discrimination and mesophyll conductance to CO₂ diffusion dynamically at different CO₂ concentrations. *Plant, Cell and Environment* **34**, 580–591.

Valentini R, Epron D, De Angelis P, Matteucci G, Dreyer E. 1995. In-situ estimation of net CO₂ assimilation, photosynthetic electron flow and photorespiration in Turkey Oak (*Quercus cerris* L) leaves—diurnal cycles under different levels of water-supply. *Plant, Cell and Environment* **18**, 631–640.

von Caemmerer S. 2000. *Biochemical models of leaf photosynthesis*. Collingwood, Australia: CSIRO Publishing .

Vrabi D, Vaskova M, Hronkova M, Flexas J, Santrucek J. 2009. Mesophyll conductance to CO₂ transport estimated by two independent methods: effect of variable CO₂ concentration and abscisic acid. *Journal of Experimental Botany* **60**, 2315–2323.

Warren C. 2006. Estimating the internal conductance to CO₂ movement. *Functional Plant Biology* **33**, 431–442.

Warren CR. 2008. Stand aside stomata, another actor deserves centre stage: the forgotten role of the internal conductance to CO₂ transfer. *Journal of Experimental Botany* **59**, 1475–1487.